JMEPEG (2011) 20:82–89
DOI: 10.1007/s11665-010-9649-6

1059-9495/$19.00

Tensile and Impact Toughness Properties of Gas Tungsten Arc Welded and Friction Stir Welded Interstitial Free Steel Joints

A.K. Lakshminarayanan and V. Balasubramanian

(Submitted June 20, 2009; in revised form January 20, 2010)

Welded regions of interstitial free (IF) steel grades in the vicinity of weld center exhibits larger grains because of the prevailing thermal conditions during weld metal solidification. This often causes inferior weld mechanical properties. In the present study, tensile properties, charpy impact toughness, microhardness, microstructure, lowest hardness distribution profile, and fracture surface morphology of the gas tungsten arc welded (GTAW) and friction stir welded joints were evaluated, and the results are compared. From this investigation, it is found that friction stir welded joint of IF steel showed superior tensile and impact properties compared with GTAW joint, and this is mainly due to the formation of very fine, equiaxed microstructure in the weld zone.

Keywords friction stir welding, gas tungsten arc welding, impact toughness, interstitial free steel, tensile properties

1. Introduction

Friction stir welding (FSW) process has emerged as a promising solid-state welding process with encouraging results. This welding technique has significant application in different fields including the automotive and the aerospace industries. While most of the FSW efforts till date have involved joining of aluminum alloys, there is considerable interest in extending this welding technology to join other materials, including steels. FSW appears to offer several advantages over arc welding of steels. The lower apparent energy inputs of FSW are expected to minimize grain growth in the HAZ, limit distortion, and residual stress in steels, eliminate welding fumes and hydrogen-induced cracking, etc. (Ref 1). However, the FSW of steels has not progressed as rapidly as aluminum for many reasons. First, the material from which the tool is made has to survive much more strenuous conditions because of the strength of steel. Second, there are also numerous ways in which steel can be satisfactorily and reliably welded. Third, the consequences of phase transformations accompanying FSW have not been studied in sufficient depth. Finally, the variety of steels available is much larger than for any other alloy system, requiring considerable experiments to optimize the weld for a required set of properties (Ref 2).

A.K. Lakshminarayanan and **V. Balasubramanian,** Department of Manufacturing Engineering, Annamalai University, Annamalai Nagar 608 002 Tamil Nadu, India. Contact e-mails: akln2k2@yahoo.com and visvabalu@yahoo.com.

Interstitial free (IF) steels with very low carbon and nitrogen contents have been successfully developed in order to perform specific or complex deep drawing operations in the automotive industry. For these grades, however, the appearance of unusually (excessive) large grain in the vicinity of the weld region of gas tungsten arc welded (GTAW) and laser welded (LW) joints has been reported (Ref 3). The presence of such zone leads to a decrease in tensile and fatigue properties of these joints (Ref 4). Since FSW is a solid-state welding process, significant differences compared to conventional welding may be expected in terms of heat-affected zone (HAZ) size and microstructure, and residual stress fields around the weld (Ref 5). Fujii et al. (Ref 6) investigated the FSW of IF steel and reported that the microstructure and mechanical properties do not significantly change due to the ultra-low carbon content, although a series of welding condition was used. However, no systematic study and detailed comparison have been reported so far on tensile and impact properties of GTAW and FSW joints of IF steel. Hence, in this investigation, an attempt was made to evaluate the tensile properties, charpy impact toughness, microhardness, microstructure, lowest hardness distribution profile (LHDP), and fracture surface morphology of GTAW and FSW joints of IF steel.

2. Experimental Procedure

The rolled plates of 4 mm thickness IF steel were cut into the required dimensions (300 mm × 150 mm) by abrasive cutting. The chemical composition of the base metal (Table 1) was obtained using a vacuum spectrometer (ARL, model 3460) by igniting sparks at various locations, and their spectrum was analysed to estimate the alloying elements. Square butt joints were fabricated autogenously (without filler metal addition) using GTAW and FSW processes. Direction of welding was normal to the rolling direction. All necessary care was taken to

Table 1 Chemical composition (mass%) of base metal

Steel	C	Mn	S	P	Si	Al	Cr	Ni	Ti	Nb	N	Fe
IF	0.002	0.05	0.007	0.007	0.011	0.046	0.019	0.012	0.07	0.001	0.0028	Bal.

Table 2 Welding conditions and process parameters

Parameters	Process	
	GTAW	FSW
Welding machine	Lincoln, USA	RV Machine Tools, India
Tungsten electrode diameter, mm	3	···
Voltage, V	20	···
Current, A	165	···
Welding speed, mm/min	70	50
Heat input, kJ/mm	2.12	0.84
Shielding gas	Argon	···
Gas flow rate	16 L/min	···
Tool rotational speed, rpm	···	800
Axial force, kN	···	7
Tool pin profile	···	Straight cylindrical
Tool shoulder diameter, mm	···	16
Pin diameter, mm	···	5
Pin length, mm	···	3.7

avoid joint distortion and the joints were made with applying suitable clamps. A nonconsumable, rotating tool made of tungsten-based alloy was used to fabricate FSW joints. Trial experiments were carried out and specimens cut at various sections of joint were subjected to macrostructural analysis. The absence of defects and full penetration was considered as the optimized condition. Also, care was taken to avoid the tool pin failure and control the heat input by controlling the combination of rotational and welding speed. The welding conditions and optimized process parameters presented in Table 2 were used to fabricate the joints for further investigation. An indigenously designed and developed CNC-controlled FSW machine (Fig. 1a) was used in position control mode to fabricate the FSW joint. The appearance (Fig. 1b) during FSW of IF steel indicates that the temperature reached during welding is approximately 900 °C. The photograph of tungsten-based alloy tool before and after FSW of IF steel is displayed in Fig. 1c. Figure 1d shows the fabricated GTAW and FSW joints. There are no macrolevel defects observed in both the joints (Fig. 2). The welded joints were sliced using abrasive cutting

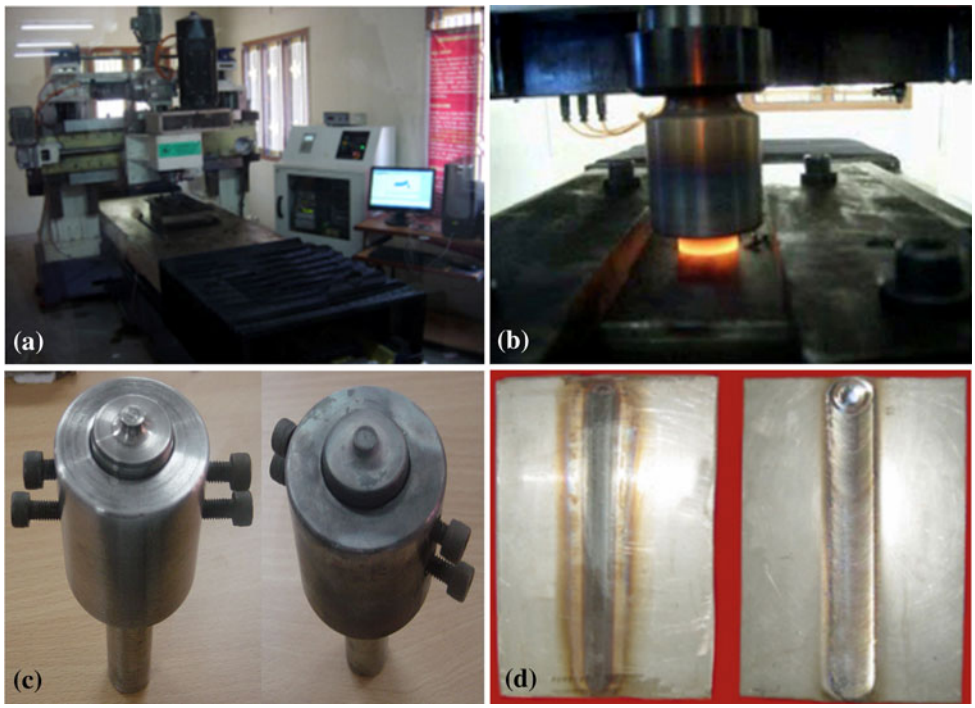

Fig. 1 (a) CNC FSW machine (6 ton, 22 kW, 4000 rpm). (b) Appearance during FSW of IF steel. (c) Tool before and after FSW of IF steel. (d) Fabricated GTAW and FSW joints

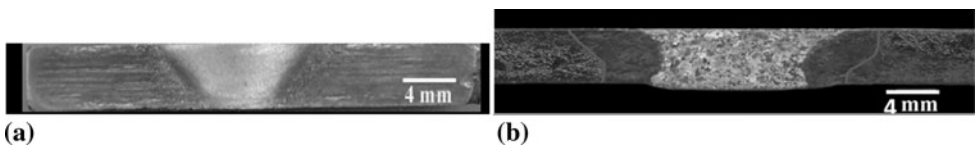

Fig. 2 Macrostructure of IF steel joints. (a) FSW and (b) GTAW

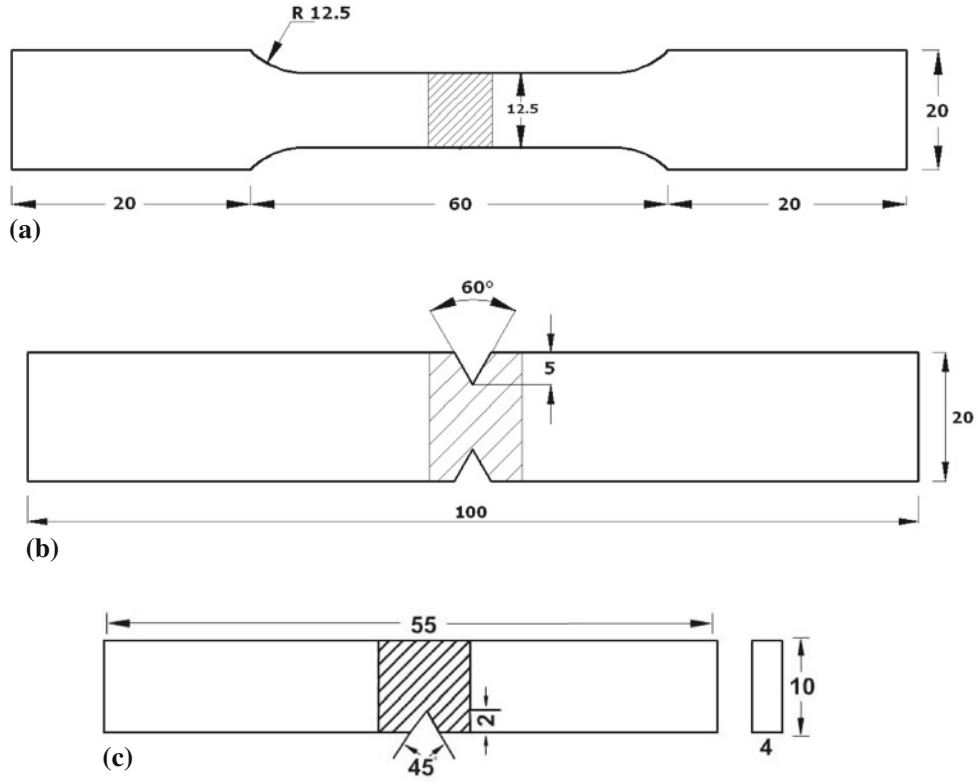

Fig. 3 Dimension of tensile and impact specimens. (a) Unnotched tensile specimen. (b) Notched tensile specimen. (c) Subsize impact specimen

Fig. 4 Photographs of tensile specimens

and then machined to the required dimensions as shown in Fig. 3. American Society for Testing and Materials (ASTM E8M-04) guidelines was followed for preparing the tensile test specimens. Two different tensile specimens were prepared to evaluate the transverse tensile properties. The smooth (unnotched) tensile specimens (Fig. 3a) were prepared to evaluate yield strength, tensile strength, and percentage of elongation. Notched specimens (Fig. 3b) were prepared to evaluate notch tensile strength (NTS) and notch strength ratio (NSR) of the joints. Tensile specimens extracted from the welded joints are presented in Fig. 4. Tensile testing was carried out using a 100 kN, electro-mechanical controlled Universal Testing Machine (FIE-Bluestar, India; Model: UNITEK-94100) with a crosshead speed of 0.5 mm/min at room temperature.

Charpy impact specimens were prepared as per the dimensions shown in Fig. 3c to evaluate the impact toughness of the weld metal and hence the notch was placed (machined) at the weld metal (weld center). Since plate thickness is small, subsize impact specimens were prepared. Impact test was conducted at room temperature using pendulum-type impact testing machine (Enkay, India; Model: Pendulam type) with a maximum capacity of 300 J. The amount of energy absorbed in fracture was recorded, and the absorbed energy is defined as the impact toughness of the material. Three specimens were tested, and the average values are given in Table 3. Vicker's microhardness tester (Shimadzu, Japan; Model: HMV-2T) was used for measuring the hardness of the weld metal with a 0.05-kg load for 15 s. Microstructural examination was carried out using a light optical microscope (MEJI, Japan; Model: MIL-7100) incorporated with an image analyzing software (Metal Vision). The specimens for metallographic examination were sectioned to the required size from the joint comprising weld metal, HAZ and base metal regions, and polishing was carried out using different grades of emery papers. Final polishing was carried out using the diamond compound (1 μm particle size) in the disc polishing machine. Specimens were etched with 2% Nital to reveal the micro- and macrostructure. The fractured surface of the tensile and impact-tested specimens was analyzed using a scanning electron microscope (JEOL, Japan; Model: 5610LV) at higher magnification to study the fracture morphology to establish the nature of the fracture.

Table 3 Transverse tensile and impact properties of welded joints

Joint type	Yield strength, MPa	Ultimate tensile strength, MPa	Elongation, %	Notch tensile strength, MPa	Notch strength ratio, NSR	Impact toughness, J	Joint efficiency, %
Basemetal	228 (2.52)	282 (2.08)	53 (3.52)	316 (2.00)	1.12	31 (0.58)	...
GTAW	173 (3.06)	208 (2.60)	30 (1.00)	199 (2.84)	0.96	17 (1.52)	74
FSW	215 (2.64)	274 (2.00)	46 (1.73)	302 (2.12)	1.10	28 (1.12)	97

Numbers given in brackets are standard deviation of experimental results

3. Results

3.1 Tensile Properties

In each condition, three specimens were tested, and the average of the three results is presented in Table 3. The yield strength, tensile strength, and elongation of GTAW joint are lower than FSW joint. The NSR of GTAW joint is 0.96. This suggests that the GTAW joint are more sensitive to notches. However, the NSR of FSW is greater than 1 and this reveals that the joints are less sensitive to notches and hence they fall into the "notch ductile materials" category. Notch tensile strength of the GTAW joint is 12% lower than the FSW joint. Joint efficiency is the ratio between tensile strength of welded joint and tensile strength of the unwelded parent metal. FSW joint exhibits 23% higher joint efficiency than GTAW joint.

3.2 Impact Toughness

Charpy impact toughness of the GTAW and FSW joints was evaluated and presented in Table 3. The impact toughness of unwelded base metal is 31 J, but the impact toughness of GTAW joint is 17 J. This indicates that there is a reduction of 45% in toughness value compared to the base metal. However, the impact toughness of FSW joint is 28 J which is only 9% lower than base metal. Of the two joints, the FSW joint exhibited higher impact toughness values, and the enhancement in toughness value is approximately 39% compared to GTAW joint.

3.3 Hardness and Microstructure

The hardness across the weld cross section was measured using a Vickers microhardness testing machine. The weld region hardness of the GTAW joint is greater than the HAZ region and lower than the base metal. In case of FSW joint, the weld metal region exhibited higher hardness than the HAZ and base metal regions. The hardness of base metal (unwelded parent metal) is 118 Hv; however, the hardness of the GTAW joint at the weld region is 94 Hv. This indicates that the hardness is decreased to 24 Hv in GTA weld region due to grain growth. The hardness of the FSW joint in the weld region is 134 Hv, and it is 40 and 16 Hv higher compared to GTAW joint and base metal, respectively. This is mainly due to the formation of very fine grains in the stir zone caused by severe plastic deformation during friction stirring.

Microstructures of both the joints were examined at different locations and they are displayed in Fig. 5. From the micrographs, it is understood that there is an appreciable difference in grain size (average grain diameter) in the weld regions. Hence, an attempt was made to measure the average grain diameter of the weld region of both the joints applying Heyn's line intercept method (Ref 7). The measured average grain diameter of base metal is 20 μm, but the average grain diameter of weld region of FSW joint is 8 μm. This indicates that there is a 12 μm reduction (refinement) in grain diameter due to the FSW process compared to base metal. Similarly, the measured average grain diameter of fusion zone of GTAW joint is 34 μm and this indicates that there is a 14 μm increase (growth) of grain diameter due to GTAW process.

Of the two techniques, the FSW process produced finer grains in the weld region compared to the GTAW process. The measured average grain diameter of HAZ of GTAW is 115 μm, but the average grain diameter of HAZ of FSW is 24 μm and this also indicates that enormous grain growth takes place in HAZ of GTAW joint compared to FSW joint. It was also observed that the width of HAZ of GTAW joint is six times larger than the width of the HAZ of FSW joint (Fig. 2). The approximate composition of elements (except carbon and nitrogen) present in the stir zone were analyzed using element distribution spectrum (EDS) indicates the evidence of tungsten particle inclusion in the stir zone microstructure and it is stemmed from the tool wear (Fig. 6).

3.4 Lowest hardness distribution profile

Generally, in welded joints, the failure location will be the weakest region (lowest hardness). Almost in all the literature, the hardness profile was measured either along the mid-thickness of joint or along the top of the plate to determine the lowest hardness regions. However, it should be pointed out that such hardness profiles could not predict the actual fracture path of welded joints because of limited data points (Ref 8). Hence, in this investigation, the hardness was measured throughout the cross section of weldment at 1 mm interval in thickness as well as in length direction. These data points were used to construct hardness distribution profile, and they are presented in Fig. 7(a) and (b), respectively, for friction stir welded and gas tungsten arc welded IF joints. Irrespective of welding processes, the lowest hardness was observed in the HAZ and it is due to the grain coarsening observed in this region. It is observed that the fracture path of welds (Fig. 7a and b) are consistent with the LHDP.

3.5 Fracture Surface

The fracture surface of tensile and impact specimens of welded joints were analyzed using SEM to reveal the fracture surface morphology. Figure 8 displays the fractographs of tensile specimens and impact specimens. The fractographs of tensile (Fig. 8a and c) and impact (Fig. 8d and f) specimens of base metal and FSW joint show ductile fracture (presence of dimples), where as, GTAW joint (Fig. 8b and e) shows brittle-like fracture (presence of cleavage facets). Fine dimples are characteristic feature of ductile fracture and hence the FSW

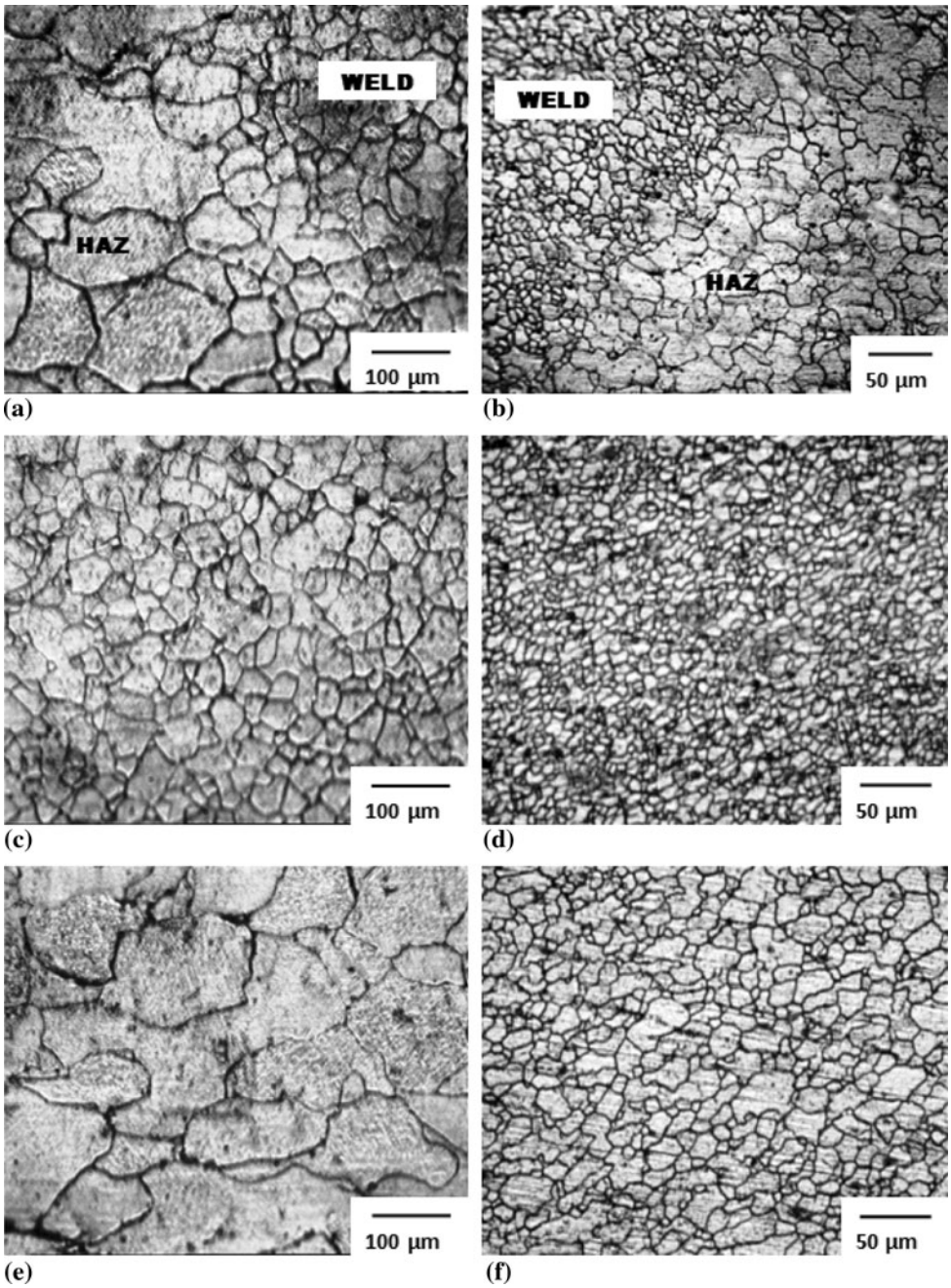

Fig. 5 Optical micrographs of IF steel joints. (a) GTAW-Weld-HAZ-Interface, (b) FSW-Weld-HAZ-Interface, (c) GTAW-Weld, (d) FSW-Stir zone, (e) GTAW-HAZ, and (f) FSW-HAZ

joints have shown higher ductility compared to GTAW joint (Table 3).

4. Discussion

Transverse tensile properties and impact toughness of the welded joints presented in Table 3 indicate that the FSW joints are exhibiting superior tensile properties compared to GTAW joints. During tensile test, all the specimens invariably failed at the HAZ of GTAW joints and at the HAZ (advancing side) of FSW joints. This suggests that the HAZ is comparatively weaker than other regions and hence the joint properties are controlled by HAZ region microstructure. The optical micrographs taken at various regions such as weld region, HAZ, and weld-HAZ interface region are presented in Fig. 5. Of the two welding processes used, GTAW process produced coarser grains compared to FSW process. Weld region and HAZ of GTAW joints primarily contain coarse grained ferrite microstructure (Fig. 5c and e), and this may be due to the excessive grain growth caused by welding heat. Naturally, the presence of such zone could decrease the tensile and impact toughness properties. The SEM fractrographs of tensile and impact-tested GTAW joint display intergranular fracture surface in which the facet size almost corresponds to the grain size (Fig. 8b and d).

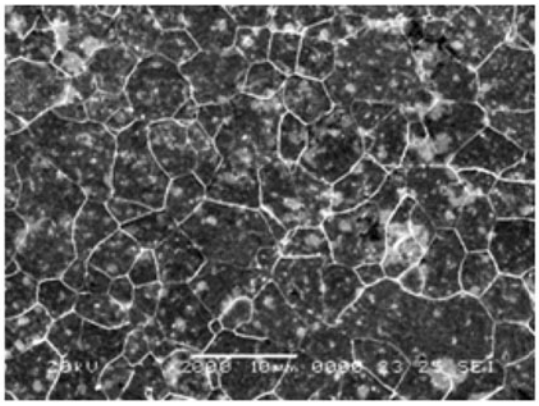

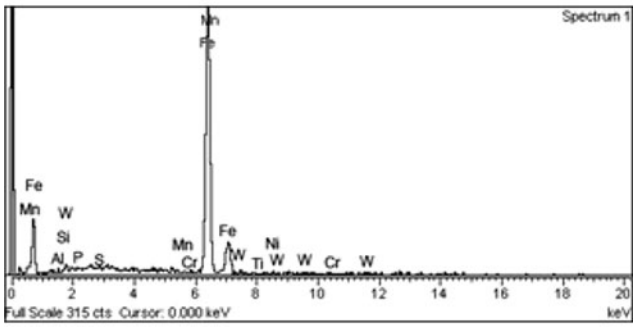

Element	Weight%	Atomic%
Al K	0.45	0.72
Si K	0.12	0.21
P K	0.08	0.11
S K	0.07	0.1
Ti K	0.81	0.92
Mn K	0.6	0.58
Cr K	0.18	0.21
Ni K	0.14	0.16
Fe K	97.26	96.8
W M	0.29	0.19
Totals	100	100

Fig. 6 SEM micrographs and EDS spectrum results of stirzone

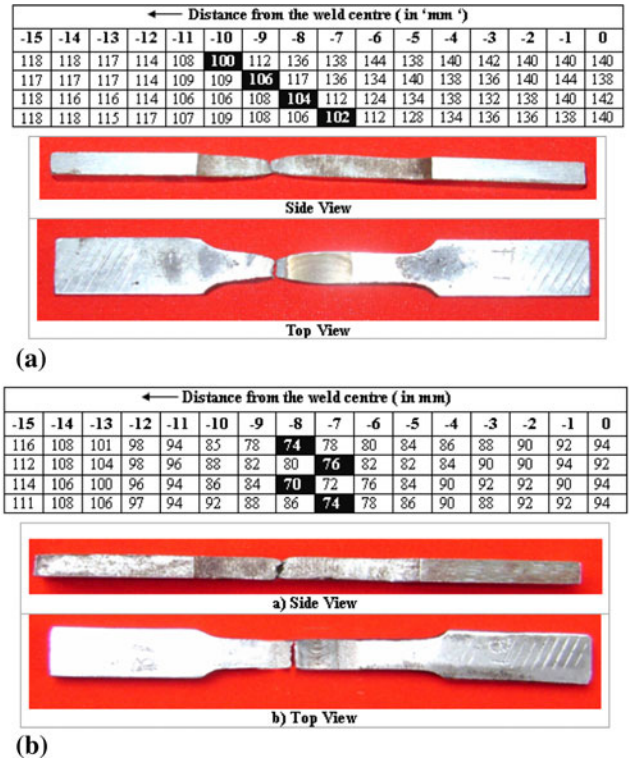

Fig. 7 (a) LHDP and fracture path of FSW joints. (b) LHDP and fracture path of GTAW joints

In GTAW joint, the region very adjacent to the fusion zone region undergoes softening and yielded lowest hardness compared to the FSW process. This is also evident from the LHDP shown in Fig. 7. The softening characteristics is influenced by the weld thermal cycles or in other words by heat input supplied by the welding process. Of the two welding processes used in this investigation to fabricate the joints, the GTAW process utilized higher heat input to weld IF steel compared to the FSW process. The net heat input (Ref 9, 10) was calculated for both processes and presented in Table 2. The variation in heat input of the welding processes influences the weld thermal cycle and subsequently causes difference in microstructural features and hardness characteristics of weld region and HAZ.

Bayraktar et al. (Ref 11) reported that heating and cooling phases of GTAW process are not simultaneous over the weld. In other words, at a given moment, certain points are in the heating phase whereas the others in the cooling phase. It is also known that for a given point along the weld line, the thermal cycle is characterized by a heating phase followed by a cooling phase. The ferrite will form far away from the fusion line and nucleates progressively at points closer to the fusion line, until austenite disappears. A very narrow edge of fine grains is observed at the vicinity of the fusion zone in the intercritical domain. Certain of these grains were found to develop at the expense of the others. The oriented growth occurs preferentially following the thermal gradient initially, unless ferrite nucleation occurs in the high temperature zones. It means that the grain growth zone associated with welding develops from the new ferrite nuclei after the passage through the intercritical domain. Certain nuclei, whose fast growth direction corresponds to the thermal gradient, will develop preferentially. As the thermal gradient increases, the growth mechanism is favored and the ferrite grain size becomes larger. Nevertheless many of the results published in the literature suggest that excessive grain growth is essentially due to recrystallization in the ferrite phase at temperatures below AC1 (Ref 12). Ductility falls off sharply at a critical test temperature with an associated rise in flow stress due to extreme microstructural instability (i.e., grain growth, Ref 13).

On the other hand, FSW process is a solid-state process in which there is no possibility of formation of molten weld pool and can inhibit the grain growth because of relatively lower heat input characteristics of the process. In FSW, frictional heat is generated between the tool shoulder and the base metal causes the material beneath the rotating tool attains a plastic state. The axial force applied through the rotating tool causes the plasticized metal to extrude around the tool pin in the vertical direction and get consolidated in the back side when the tool moves forward. Both the stirring and extrusion cause the elongated grains to fragment into smaller grains, and this replaces the original base metal grain structure into a very fine

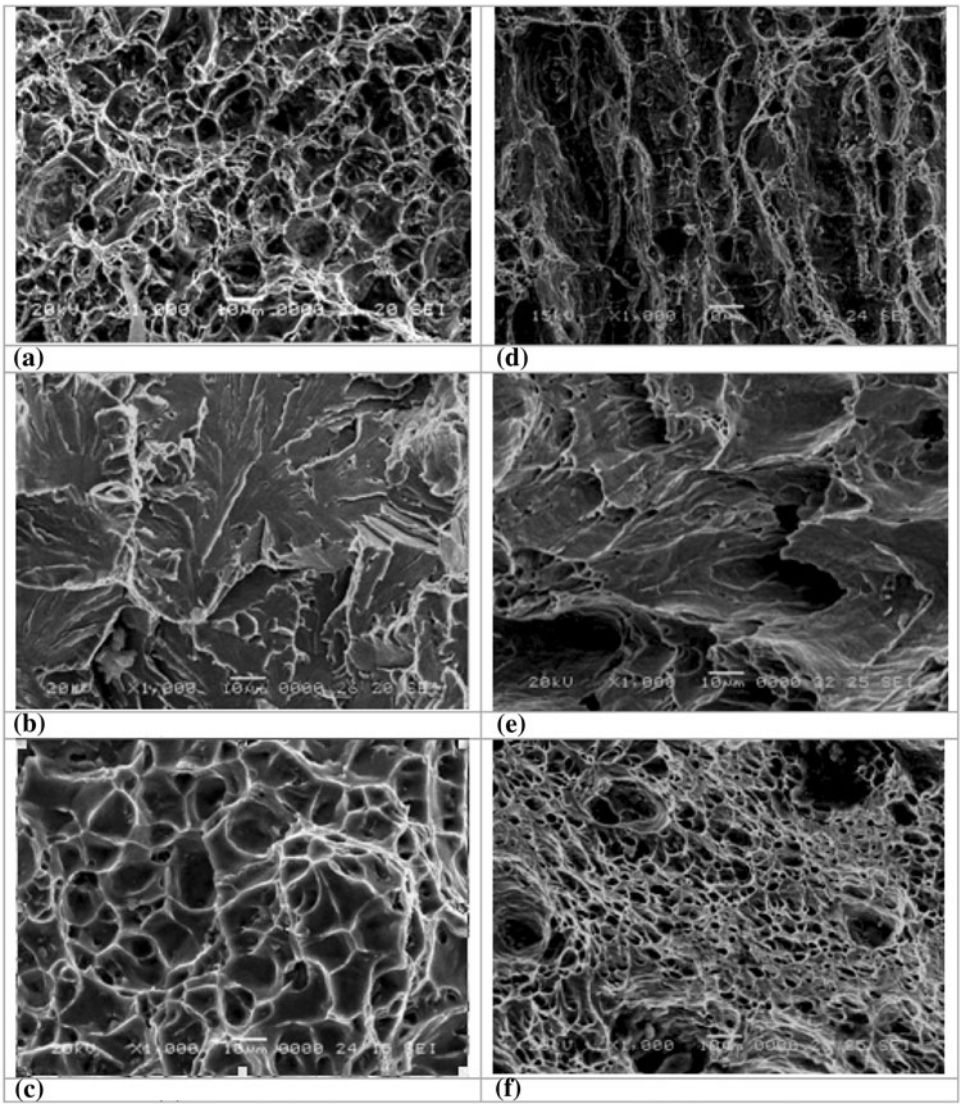

Fig. 8 SEM fractographs of tensile and impact specimens. (a) Basemetal-Tensile, (b) GTAW-Tensile, (c) FSW-Tensile, (d) BM-Impact, (e) GTAW-Impact, and (f) FSW-Impact

equiaxed grain structure in Stirzone. The SEM fractrographs of tensile and impact-tested FSW joint shows finer dimples corresponds to the grain size (Fig. 7c and f). The variations of the temperature values are limited by the melting point of the welding material and the maximum temperature ranges from 80% to 90% of the melting point. The peak temperature measured during FSW of IF steel was around 900 °C, and it revealed that the IF steel was welded in the ferrite single-phase region, and no transformation occurred (Ref 14). Fuji et al. (Ref 14) reported that FSWs give rise to a large plastic flow in the stir zone, which causes the introduction of many dislocations and grain subdivision by the dislocations boundaries to evolve fine grained microstructure. The dislocations and fine grains contribute to the strengthening of the stir zone. The decrease in grain size increases the strength with significant reduction in ductility. However, the formation of fine, equiaxed grains and relatively higher hardness and ductility are the reasons for superior tensile and impact properties of FSW joints compared to GTAW joints.

5. Conclusions

In this investigation, the tensile and impact toughness properties of GTAW and FSW joints of IF steel were evaluated and the following important conclusions are derived:

- Of the two welded joints, the joints fabricated by FSW process exhibited higher strength values and the enhancement in strength is approximately 24% compared to joint fabricated by GTAW process.
- Of the two welded joints, the joints fabricated by FSW process exhibited higher impact toughness values and the enhancement in toughness is approximately 39% compared to the joint fabricated by GTAW process.
- The formation of fine, equiaxed grains and relatively higher hardness of weld region and HAZ are the reasons for superior tensile and impact properties of FSW joints compared to GTAW joints.

Acknowledgments

The authors thank Clean Technology Division, Ministry of Environment and Forest, New Delhi for financial support to carry out this investigation through sponsored project MOEN No. 1-9/2005-CT. The authors also thank to Dr. S. Chatterjee, Professor, Bengal Engineering College, Calcutta for providing the IF steel material to carryout this investigation. In addition, we thank the referees and the editor for constructive feedback.

Appendix 1

Heat Input Calculations of Processes Used

Gas Tungsten Arc Welding.

$$\text{Heat Input} = \frac{V \times I \times \eta \times 60}{S \times 1000} = \frac{165 \times 20 \times 0.75 \times 60}{70 \times 1000} = 2.12\,\text{kJ/mm}$$

where V is the voltage in volts; I, current in Amps; and η, arc efficiency is assumed as 0.75 for GTAW (Ref 9).

Friction Stir Welding. The heat input for FSW process can be calculated as (Ref 10)

$$q = \frac{2\pi}{3S} \times \mu \times p \times \omega \times R_S \times \eta = \frac{2\pi}{3 \times 0.83} \times 0.3 \times 13 \times 13.3 \times 0.008 \times 0.8 = 0.84\ \text{kJ/mm}$$

where μ is coefficient of friction; P, normal force in kN; ω, rotational speed in rev/s, and R_s, shoulder radius in m; and S, the welding speed in mm/s.

References

1. T.J. Lienert, W.L. Stellwag, Jr., B.B. Grimmett, and R.W. Warke, Friction Stir Welding Studies on Mild Steel, *Weld J.*, January, 2003, p 1s–9s
2. R. Nandan, T. DebRoy, and H.K.D.H. Bhadeshia, Recent Advances in Friction Stir Welding—Process, Weldment Structure and Properties, *Prog. Mater. Sci.*, 2008, **53**, p 980–1023
3. Y. Tokunaga and H. Kato, Application of IF Steel Sheets to Automobile Parts, *Conf. Proceedings, Metallurgy Vacuum Degassed Steel Products, Conf. Proceedings TMS*, R. Pradhan, Ed., TMS, 1989, p 91–108
4. W.M. Thomas, P.L. Threadgill, and E.D. Nicholas, Feasibility of Friction Stir Welding of Steel, *Sci. Technol. Weld. Join.*, 1999, **4**, p 365–372
5. R.S. Mishra and Z.Y. Ma, Friction Stir Welding and Processing, *Mater. Sci. Eng. A*, 2005, **50**, p 1–78
6. H. Fujii, L. Cui, N. Tsuji, M. Maeda, K. Nakata, and K. Nog, Friction Stir Welding of Carbon Steels, *Mater. Sci. Eng. A*, 2006, **429**, p 50–57
7. "Standard Test Methods for Determining Average Grain Size," ASTM E112-04, 2006, p 13–14
8. S.R. Ren, Z.Y. Ma, and L.Q. Chen, Effect of Welding Parameters on Tensile Properties and Fracture Behavior of Friction Stir Welded Al-Mg-Si Alloy, *Scr. Mater.*, 2007, **56**, p 69–72
9. G. Atkins, D. Thiessen, N. Nissley, and Y. Adonyi, Welding Process Effects in Weldability Testing of Steels, *Weld. J.*, April, 2002, p 61s–68s
10. A.K. Lakshminarayanan, V. Balasubramanian, and K. Elangovan, Effect of Welding Processes on Tensile Properties of AA6061 Aluminium Alloy Joints, *Int. J. Adv. Manuf. Technol.*, 2009, **40**, p 286–296
11. E. Bayraktar, D. Kaplan, L. Devillers, and J.P. Chevalier, Grain Growth Mechanism During the Welding of Interstitial Free (IF) Steels, *J. Mater. Process. Tech.*, 2007, **189**, p 114–125
12. D.O. Wilshynsky, G. Krauss, and D.K. Matlock, Recrystallisation Behavior of IF Sheet Steels, *Conf. Proceedings*, L.E. Collins and D. Baragar, Ed., CANMET, Canada, 1991, p 69–79
13. E. Bayraktar, D. Kaplan, C. Buirette, and M. Grumbach, Application of Impact Tensile Testing to Welded Thin Sheets, *J. Mater. Process. Tech.*, 2004, **145**, p 27–39
14. H. Fujii, U. Rintaro, C. Ring, K. Nakata, and K. Nogi, Friction Stir Welding of Ultrafine Grained IF and Carbon Steels, *Trans. JWRI.*, 2006, **35**, p 47–52